Enhancing Zinc-Rich Epoxy Ester Coatings: Optimizing Corrosion Resistance with Functional Pigments

Zlepšení epoxidových esterových povlaků bohatých na zinek: Optimalizace odolnosti proti korozi pomocí funkčních pigmentů

Raycha Y., Kohl M., Kalendová A.

Faculty of Chemical Technology, University of Pardubice, Pardubice, Czech Republic, yash.raycha@student.upce.cz

Summary

It was investigated how various particle kinds, sizes, and characteristics affected the mechanical and corrosion resistance of pigmented systems that contained spherical zinc. Members of the transition metal dichalcogenide (MoS₂) group, metallic pigments such as Al and Mg, conductive polymers such as polyaniline-PTSA, inorganic oxides such as MgO, organometallic anticorrosive pigment such as OP-Mg, and other semiconductor materials such as ZnS were employed in this study. These particles' multilayer, ultra-thin structure was designed to offer improved mechanical and anticorrosion properties. These particles' modes of action in heterostructure hybrid coating systems were clarified. Optimum dosage of these materials in combination with spherical zinc metallic pigments was to be determined with increased performance in chemical, corrosion and mechanical properties.

Key words: Conductive polymers; zinc, aluminium and magnesium metallic pigments; epoxy ester coating; organic anticorrosive pigments; inorganic oxides and sulphides; anticorrosion performance.

1. Introduction

Corrosion is a slow chemical or electrochemical process in which a metal interacts with a corrosive medium (water, oxygen, chloride ions, etc.), resulting in the loss of its original properties such as high hardness, strength, and lustre, leading to huge economic losses and social impacts. The most common and versatile method of protecting metallic materials from corrosion is the application of organic coatings, which protect the metal substrate through four mechanisms - barrier, adhesion, inhibition, and electrochemical action. The combination of these four mechanisms in the coating film leads to the resulting corrosion protection [1-4].

Basic zinc-pigmented coatings use electrochemical, filtration, and neutralization protection mechanisms in addition to the barrier effect for corrosion protection of metallic materials, most often steel. However, the zinc particles in zinc pigmented protective organic coatings protect the steel substrate electrochemically (cathodic protection) only in the first phase of its action. Zinc is electrochemically less noble than steel or iron, and if the connection

between the individual zinc particles and the zinc coating and the steel is sufficiently conductive, mutual polarization will occur. The zinc contained in the coating film thus becomes the anode and the steel substrate the cathode. In the event of a breach in the coating film and electrolyte penetration, cathodic protection is triggered at the point of breach, the zinc begins to oxidize, and its corrosion products begin to heal the breached area. The corrosion fumes thus perfectly seal all cracks and pores in the coating film, resulting in a very compact and perfectly adhesive layer applying a barrier protection mechanism that is resistant to normal atmospheric influences. The barrier mechanism is strengthened by a filtering and neutralizing mechanism/effect, which results in the separation of oxygen or other corrosion stimulants (Cl., SO₄²⁻) from the electrolyte penetrating the undamaged zinc-pigmented coating film. As a result of the reaction of these corrosion stimulators with the zinc metal particles present in the coating film, zinc corrosion products are formed, which reinforce the barrier mechanism. Although zinc coatings are less toxic compared to coatings containing lead or chromate compounds, zinc corrosion products are classified as hazardous to the aquatic environment. For this reason, there are efforts to reduce the zinc content of coatings with other non-toxic pigments to achieve high corrosion protection [5-12].

Two-dimensional (2D) materials belong to a large and diverse class of single-layer carbonaceous materials, dichalcogenides, phosphides, nitrides, halides, one or more layered transition metal oxides, and layered silicate materials [13-15]. These materials are exceptional due to their unique physical and chemical properties, structural diversity, large surface area-to-volume ratio, and good electrical conductivity, which make them applicable in a number of industrial areas - optics, electronics, catalysis, sensors, and power units. (batteries, supercapacitors, or solar cells) [16-18]. Two-dimensional materials have recently attracted more attention in the field of anti-corrosion protection [19].

Transition metal dichalcogenides are 2D layered materials with ultrathin structures whose properties are highly dependent on the degree of crystallinity, number of layers, and layering sequences in their crystals and thin films [15, 20]. With the growing interest in layered transition metal dichalcogenides, MoS₂ has taken a unique place due to its exceptional properties and structure as a graphene analogue. Layers of molybdenum atoms are arranged in a hexagonal array sandwiched between layers of sulfur, which are held by strong covalent bonds, while Van der Waals interactions exist between the sulfur layers. Due to this unique lamellar structure, MoS₂ has good corrosion resistance like graphene. Still, unlike graphene,

MoS₂ is a semiconductor with a relatively high forbidden band and, therefore, has no effect on the electrical conductivity of the epoxy resin [15, 19-22].

Single or multi-layer transition metal oxides have a relatively long history, are found in many minerals, and are widely used as construction materials, pigments, lubricants, and in many other applications. In single or multilayer oxides, the transition metal electrons are strongly attracted to oxygen, and consequently, their physical, chemical, and structural properties are strongly determined by the correlated d electrons. These materials exhibit different physical and chemical properties compared to their bulk counterparts, giving rise to several remarkable properties such as high-temperature superconductivity, multiferroicity, and unique optical, mechanical, and thermal phenomena [13, 27]. Magnesium oxide (MgO) is an important inorganic pigment used in paints and coatings due to its unique physical and chemical properties. Known for its high thermal stability, whiteness, and excellent dispersibility, MgO enhances the brightness and opacity of paint formulations. Its alkaline nature contributes to its anticorrosive capabilities, as it can neutralize acidic environments and inhibit the growth of rust on metal surfaces. Additionally, MgO provides a protective barrier that reduces moisture penetration and improves the durability of coatings, particularly in harsh industrial and marine environments. It is widely employed in both primer and topcoat systems, especially in corrosion-resistant paints for steel structures, pipelines, and reinforced concrete. Due to its costeffectiveness and multifunctional role, MgO continues to be a valuable component in modern protective coatings. [28-30]

Other important semiconductors include zinc sulfide. Zinc sulfide N-type semiconductor material possessing a high refractive index, high dielectric constant, and unique photocatalytic properties. Due to its high refractive index, it finds application as a pigment in UV-curable coatings and for the production of photodetectors and photodiodes. ZnS is also used as an additive in plastics, where it serves as a flame retardant [38-40]. ZnS, together with BaSO₄, is also represented in litopone, which is produced by coprecipitation and subsequent calcination of a mixture of zinc sulfide and barium sulfate (ZnS content = 30 %). This type of pigment combines the individual advantages of both types of compounds and is used in paint formulations [31,32].

Aluminum (Al) and magnesium (Mg) metal powder pigments are widely used in anticorrosive paint formulations due to their excellent electrochemical properties and barrier effects. Both metals possess high anodic potentials, which allow them to function as sacrificial anodes when applied to steel substrates. This means they corrode preferentially, protecting the

underlying metal from oxidation through galvanic action. Aluminum pigments also form a dense, reflective barrier that limits oxygen and moisture diffusion, enhancing long-term durability. Magnesium, being more reactive, provides strong cathodic protection in aggressive environments, especially when rapid passivation is not required. When used in combination with zinc metallic pigments, these powders improve the overall protective performance by extending the galvanic protection range. Zinc offers the most effective sacrificial protection, while Al and Mg help reinforce the barrier and prolong coating life. This synergistic blend is especially effective in heavy-duty primers for marine, automotive, and industrial steel structures.[33-35]

Currently, the commonly used environmentally friendly corrosion inhibitors include organic compounds containing heteroatoms and π electrons [36-38], for example imidazoline, thia-diazole derivatives, amino acid or sulfhydryl compounds. Organic pigments are substances with distinct colour shades, almost insoluble in water and organic solvents, and characterized by resistance to UV and visible radiation and thermal stability. For the most part, they are prepared by converting water-soluble organic dyes into insoluble organic pigments, which are created either by removing solubilizing groups from the organic dye molecule or by creating an insoluble salt by replacing soluble metal ions with less soluble ones.

A number of works also address the use of conductive polymers for their combination with zinc or even conductive polymers in the form of coated pigment particles in conductive polymer coatings. Organically synthesised polymeric compounds known as "conductive polymers" have conductivity in a range of semiconductors. They are available in powder form, making it possible to employ them in coatings. Two of the most often utilized conductive polymers are polyaniline and polypyrrole. Polyaniline, a conductive polymer that may be created in five different methods, is a notable example. Its numerous forms have different degrees of oxidation or protonation, chemical composition, stability, color, and electrical characteristics. [39-41] The anion in the polyaniline structure counteracts the chain's positive charges. The sort of anion present is determined by the protonating acid utilized. [42]

2. Experimental part

2.1. Materials

Molybdenum disulfide (MoS2), zinc sulfide (ZnS) and magnesium oxide (MgO) were from the company Merck KGaA, Darmstadt, Germany. Zinc (Zn), magnesium (Mg) and Aluminium (Al) was from the company Radka International s.r.o., Lázně Bohdaneč, Czech

Republic. Conductive polymer (PANI-PTSA) and organic anticorrosive pigment (OP-Mg) were synthesised in lab in University of Pardubice, Czech Republic. Epoxy ester resin WorléeDur D46 and sicative Valirex Mix 835 D60 were from the company 3P-CHEM s.r.o., Zbůch, Czech Republic. Loctite EA 9466 was from the company Ulbrich Hydroautomtik s.r.o., Brno, Czech Republic. Xylene, were from the company PENTA s.r.o., Prague, Czech Republic. Q-panels were from the company Q-LAB DEUTSCHLAND GMBH, Saarbrucken, Germany.

2.2. Synthesis of Mg-Organics pigments and Conductive polymers

Synthesis of Mg-Organics pigment

Diazotization of anthranilic acid

Anthranilic acid (6.85 g; 50 mmol) was mixed with 50 cm3 of water. Then 35% HCl (10.4 g; 100 mmol) was added. The mixture was externally cooled to 0–5 ° C, and aqueous 2M NaNO2 (27 cm-3) was slowly added dropwise with stirring at 0–5 °C. The formed solution of diazonium compound I (Figure 1) was immediately used for a coupling reaction.

COOH
$$NH_2 + NaNO_2 + 2 HCI$$

$$0-5^{\circ}C$$

$$COOH$$

$$N_2^{+}Cl^{-} + NaCl + 2 H_2O$$

Figure 1. Summary equation of diazotization of anthranilic acid

Coupling to 5-methyl-2-phenyl-3- pyrazolone, Dye I (C17H14N4O3)

5-Methyl-2-phenyl-3-pyrazolone (8.71 g, 50 mmol) was mixed with 80 cm3 of water and 4M NaOH (12.5 cm3) was added under the stirring. Then the formed solution was cooled at 0–5 °C and the diazonium compound I was slowly added under the vigorous stirring. The reaction pH was adjusted to value 8 (using 4M NaOH). When the coupling reaction (Figure 2) was completed, the pH was adjusted using 30% HCl to the value 1–2 (-COONa \Box -COOH). Finally, the formed yellow product (Dye I) was filtered off and washed with water to remove salts and acids. Finally, the Dye I was dried at 80 °C.

COOH
$$N_{a}^{\dagger} \overline{O}$$

$$+ NaOH$$

$$+ NaOH$$

$$0-5^{\circ}C$$

$$+ NaCI + H_{2}O$$

$$+ NaCI + H_{2}O$$

Figure 2. Summary equation of coupling reaction to Dye I

Preparation of magnesium complex Mg-Dye-I (C34H26MgN8O6)

Dye I (14.45 g, 45 mmol) was mixed with water (200 cm3) and MgCl2 (4.285 g, 50 mmol) was added. The reaction mixture was then vigorously stirred at 80 °C for 4 hours and during the reaction the pH was adjusted to 6 with NaOH solution. When the reaction (Figure 3) was completed, the reaction mixture was cooled at room temperature (22 °C) and the formed Mg-Dye-I was filtered off and washed with water to remove all salts (NaCl, etc.). The yield of Mg-Dye I was 16.69 g, (68.3 % relative to default Dye I).

Figure 3. Synthesis of Mg-Dye-I. (for simplicity, metal complex bonds are not indicated in the structural formula)

Synthesis of polyaniline polymers by oxidative polymerisation

Aniline is oxidized by ammonium peroxodisulphate in an acidic media (PTSA) to produce PANI-PTSA. The reaction (exothermic) occurs in air at room temperature. 250 ml of 0.25 M ammonium peroxodisulphate (Merck) was dissolved in distilled water, and 250 ml of 0.2 M aniline (Merck) was dissolved in 0.3 M para-toluene sulphonic acid. After combining the two solutions, the resulting liquid underwent a mechanical stir for 60 minutes. The initially colorless reaction liquid turned blue during the polymerization process before finally taking on the PANI-PTSA green hue. The mixture for the reaction was then left overnight. Using a Buchner funnel to filter off the PANI-PTSA precipitate that resulted, the product was then washed with diluted phosphoric acid and acetone. After 24 hours, the resultant PANI-PTSA powder was dried for 24 hours in air and subsequently in an oven at 60 oC.

Figure 4. Polymeric reaction of aniline to polyaniline

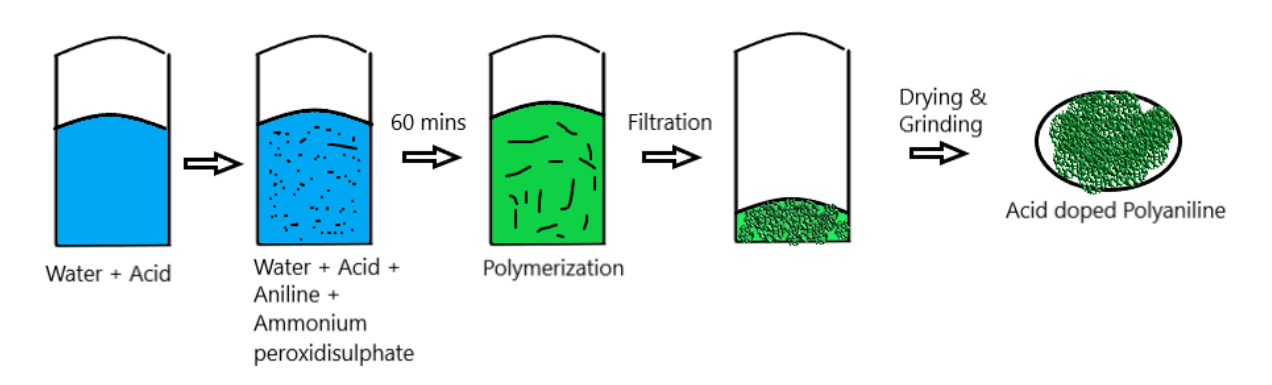


Figure 5. Graphical representation of stages of reaction of polyaniline with time

2.3. Characterization of the binder and pigments by methods used in the coatings field. Characterization and specification of the epoxy ester resin

WorléeDur D46, a commercially available epoxy ester resin, was used as a binder to make the model paint. This type of binder was specified using the following parameters: dry matter, colour according to DIN ISO 4630, acid value according to DIN EN ISO 2114, and viscosity as determined by a rheometer. Nicolet iS50's dry film binder's infrared spectroscopy (FTIR) was measured using the ATR method on the diamond crystal.

Determination of physio-chemical properties studied inorganic pigments.

A Micromeritics AutoPycnometer 1340 (Norcross, GA, USA) was used to measure the densities of eight different kinds of inorganic and organic pigments under study. The "pestlemortar" method was used to test the oil absorption of the inorganic pigments under study. The critical pigment volume concentration (CPVC) was computed using the measured outcomes of the calculations.

SEM and EDX measurements of pigments

Using a scanning electron microscope (LYRA 3; Tecan) outfitted with an EDS analyzer (Aztec X-Max-20; Oxford Instruments), elemental composition data (EDX) and scanning electron microscopy (SEM) images of the pigments under study were collected. The samples underwent measurements on five $200 \times 200 \, \mu m$ areas at a voltage of 20 kV accelerating voltage after being coated with a 20 nm carbon conductive layer (Leica ACE 200). The error bars show the standard deviations of the measured values and are the average of the results. 18 nm of gold conductive layer was applied on the pigments, and samples under study were SEM scanned at an acceleration voltage of $10 \, kV$.

2.4. Preparation of formulated model coating systems and their application

Synthesis of coatings is divided into four groups: Coatings with zinc and inorganic pigments (MgO, ZnS, MoS₂), Coatings with Zinc and metallic pigment (Al, Mg), Coatings with Zinc and conductive polymer (polyaniline-PTSA), Coatings with Zinc and organic pigment (OP-Mg).

The model paints were formulated at a combination of pigment volume concentration of studied pigments PVC = 0, 1, 3 and 5% and subsequently were model paints also pigmented with powder metal zinc with spherical particle shape to maintain a constant concentration of solids so that the pigment volume concentration to critical pigment volume concentration ratio was PVC/CPVC = 0.5.

The model paints were made using a Dissolver type apparatus (Dispermat® CN30-F2, VMA-Getzmann GMBH, Reichshol, Germany) at 2000 rpm/45 minutes using dispersion beads with a diameter of 2.85 to 3.45 mm. Valirex Mix 835 D60, a drying agent, was used at the amount recommended by the resin manufacturer (i.e., 0.1% converted to 100% alkyd resin). Valirex Mix 835 D60 is a mixed metal carboxylate based on cobalt, calcium, and zirconium that has been diluted in D60, with an overall metal composition of 8.8%. The viscosity of the prepared model paints was altered using xylene.

The created model paints, which featured specific pigments under research mixed with spherical zinc, were then used to paint standard glass and steel Q-Panels (low-carbon steel panels). ZQD-SP-104171 steel panels were used for mechanical testing, and QD24 steel panels were used for electrochemical studies. After being prepared in compliance with ISO 1514, model paint materials were applied to individual panels using a 4-sided applicator ZFR 2040.8050 (Zehntner GmbH Testing Instruments, Sissach, Switzerland). Single-layer systems with dry film thicknesses (DFT) of roughly 100 µm were produced for mechanical and electrochemical tests.

The dry thickness of paint coatings applied to glass panels was measured in accordance with ISO 2808 using a dial thickness gauge (Schut-20, Schut Geometrische Meettechniek B.V., Groningen, Netherlands). The thickness of prepared organic coatings applied to steel panels while they were drying was measured using a Byko-test 8500 premium Fe/NFe magnetic thickness gauge (BYK Additives & Instruments, Wesel, Germany). A vertical cut of 80 mm in length and 0.5 mm in width was employed for organic coatings meant for corrosion testing. Using a cutting tool (Elcometer 1538, DIN scratching tool with 1 mm Cutter, Manchester, England) that complied with ISO 2409, the vertical cuts were finished in compliance with CSN EN ISO 12944-6.

2.5. Study of the physical-mechanical and chemical resistance properties of the tested organic coatings

Using the correct instruments and following the guidelines provided by the standards, the mechanical characteristics of the studied organic coatings containing the studied pigments were assessed. A BYK-Gardner Byko-Swing (5867) Persoz Hardness Tester for Coatings (BYK-Gardner GmbH, Geretsried, Germany) was used to assess relative surface hardness in accordance with ISO 1522. The degree of adhesion was assessed using the Elcometer 1542 Cross Hatch Adhesion Tester, which is produced in Manchester, UK, in compliance with ISO 2409. The Elcometer 1615 Variable Impact Tester (Elcometer, Manchester, UK) was used to perform the rapid-deformation (impact resistance) test in compliance with ISO 6272. The bend test (cylindrical mandrel) was performed in compliance with ISO 1519 using an Elcometer 1500 Cylindrical Mandrel on a Stand (Elcometer, Manchester, UK). A cupping test in compliance with ISO 1520 was conducted using the Elcometer 1620 Cupping Tester (Elcometer, Manchester, UK). The pull-off test for adhesion was carried out using a COMTEST®OP3P in compliance with ISO 4624 (Roklan - electronic s.r.o., Prague, Czech Republic).

Score	Appearance of surface of cross-cut area from which flaking has
	occurred
0	
1	
2	
3	
4	
5	_

Figure 6. Assessment of cross cut test according to ISO 2409

The MEK (Methyl Ethyl Ketone) resistance test is a widely used method to evaluate the solvent resistance and cure level of organic coatings, particularly for coil coatings and industrial finishes. The test is typically performed according to ISO 2812-1 (or ASTM D5402) standards. A cloth soaked in MEK is rubbed back and forth over the coated surface with moderate pressure, usually for a specified number of double rubs (e.g., 25, 50, or 100). The coating's resistance is assessed by observing any softening, color removal, or film degradation. A properly cured coating should show minimal or no damage.

2.6. Corrosion test procedures and evaluation of results after corrosion tests

The salt spray test (ISO 9227) is an accelerated corrosion test used to evaluate the corrosion resistance of metallic coatings, paints, or surface treatments. Test panels are placed in a chamber where they are continuously exposed to a fine mist of salt solution (typically 5% NaCl) at 35 °C. The exposure time varies depending on the specification (e.g., 24, 96, 240, or 1000 hours). After the test, panels are visually inspected for signs of corrosion, blistering, or coating failure.

This test provides a standardized way to compare the protective performance of coatings under harsh conditions. Tests were conducted in a testing chamber (SKB 400 A-TR-TOUCH, Gebr. Liebisch GmbH & Co. KG, Germany) over the course of three 12-hour cycles: 10 hours of exposure to a mist of 5% NaCl solution at 38 °C; 1 hour of exposure at 23 °C; and 1 hour of humidity condensation at 40 °C.

According to ISO 22479, the corrosion test was carried out in a testing chamber called KB 300A (Gebr. Liebisch GmbH & Co. KG, Bielefeld, Germany) in a humid atmosphere with SO2. Eight hours of humidity with SO2 content (1000 ml of SO2 dosed into a 300 L chamber) at 38 °C came after sixteen hours of drying at 23 °C with less than 75% humidity. The test was repeated in these 24-hour cycles. The paint film samples under scrutiny were put through this corrosion test for 960 hours.



Figure 7. Salt Spray Chamber

Evaluation of the corrosion tests

Following exposure, the test panels were assessed from the perspectives of osmotic blister formation (ASTM D714-87), the degree of surface corrosion (ASTM D610-85), and the corrosion at scribe (ASTM 1654-92). Defects can be formed by diffusion of the testing environment like moisture, salt and acid fumes into the film to the substrate. Formation of blisters on the coating also has relative relationship with coatings adhesion to the substrate, the better the adhesion there is less chances of osmotic blisters

A further result of accelerated tests which is evaluated is the corrosion in cut scribe of artificially prepared mechanical disturbance of film by a cross section. Data on the electrochemical activity of the anticorrosive pigment employed in the coating are provided by the corrosion and distance of corrosion traces from the section. If the area around the part shows no signs of corrosion, the anticorrosive pigment is working to prevent cathodic or anodic corrosion.

ASTM D 714-87 method

The method classifies the osmotic blisters to the groups according to their sizes designated by numbers of 2, 4, 6, and 8 (2 denotes the largest size, 8 the smallest one). Along with size of blisters an information on the density is also given. The highest occurrence density of blisters is designated as D (dense), the lower ones as MD (medium dense), M (medium) and F (few). In such a way a series from the surface area attacked at least by the osmotic blisters up to the heaviest occurrence can be formed as follows: 8F-6F-4F-2F-8M-6M-4M-2M-8MD-6MD-4MD-2MD-8D-6D-4D-2D.

ASTM D 1654-92 method

This method evaluates the corrosion severity along the section and the degree of coating sub corroding in the vicinity of section. Rating is done from 0 to 10 mm.

ASTM D 610-85 method

The results obtained by means of this method are compared with the standards given in the Annex, which are related to the degree of corrosion in area under the protective coating. The result is thus a definite corrosion degree of the substrate surface expressed in percent (0-0.03-0.1-0.3-1-3-10-16-33-50-100 %).

Electron Microanalysis Studied Organic Coatings

The organic coatings investigated were subjected to electron microanalysis using a TESCAN VEGA 5130SB scanning electron microscope and a Bruker Quantax 200 energy dispersive X-ray spectrometer to determine the elemental composition of the organic coatings containing the studied organic and inorganic pigments after 960 hours of exposure in atmosphere salt electrolyte.

2.7. Electrochemical Measurement Linear Polarization

The linear polarization test is an electrochemical method used to assess the corrosion behavior of metals and coatings in a given environment. It measures corrosion rate and protection efficiency. A small potential (typically $\pm 20 \, \text{mV}$) is applied around the corrosion potential (Ecorr) while recording the resulting current. The slope of the current–potential curve gives the polarization resistance (Rp). From Rp, the corrosion current density (Icorr) is calculated, which is then used to estimate the corrosion rate (Vcorr), usually expressed in mm/year or mpy (mils per year).

The polarization resistance was determined from Stern-Geary equation:

$$I_{cor} = \frac{B}{R_p} \tag{1}$$

where the Rp is polarization resistance and B is a constant for the particular system which is calculated from the slopes of the anodic (β_a) and cathodic (β_c) Tafel regions:

$$B = \frac{\beta_a \,\beta_c}{2.303 \left(\beta_a + \beta_c\right)} \tag{2}$$

Corrosion rate was calculated according to the following equation, where K is constant that defines the units of the corrosion rate, EW is equivalent weight, ρ is density and A is sample

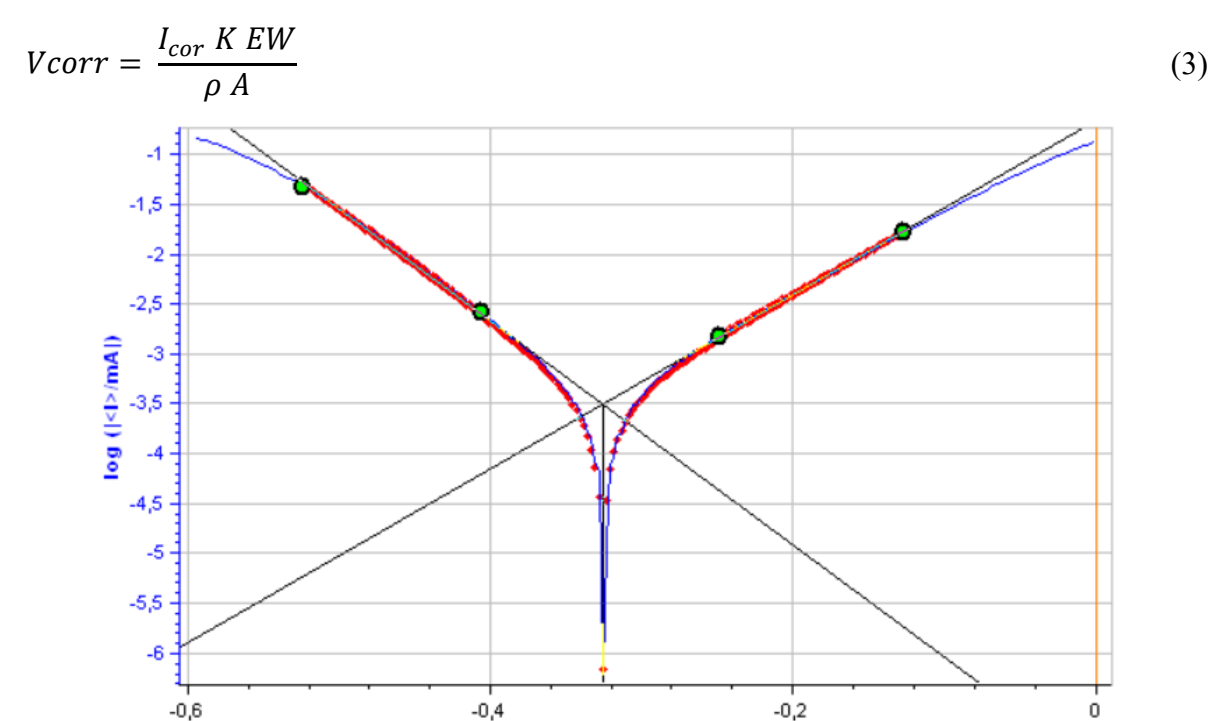


Figure 8. Tafel fit analysis

Ewe/V

Ecorr: Corrosion potential — the natural potential where corrosion occurs.

-0,4

Icorr: Corrosion current density — directly related to the corrosion rate.

Rp: Polarization resistance — indicates resistance to corrosion; higher Rp means lower Icorr.

Vcorr: Corrosion rate — the material loss over time.

-0,6

An instrument called the multichannel potentiostat/galvanostat VSP-300 (Bio-Logic, Seyssinet-Pariset, France) was used to measure the polarization curves of the examined organic coatings. Version V10.23 of the 2012 edition of the EC-Lab® software was used to assess the polarization curves. The samples were exposed to a 1 M NaCl solution in a galvanic cell (Bio-Logic, Seyssinet-Pariset, France) that had a saturated calomel electrode and a platinum working electrode. In the range of -10 mV EOC-1 to +10 mV EOC-1, One centimeter square of each distinct organic coating under study was polarized at a rate of 0.166 mV·s-1



Figure 9. Experimental set up for linear polarization test

3. Results and discussion

3.1. Specification of the used binder.

Binder specification is summarized in Table 1. The spectrum of the epoxy ester resin shown in Figure 10 was measured. In the given spectrum, a wide band of valence vibration of OH groups (hydroperoxides, alcohols, carboxyl groups) was found at 3590-3280 cm⁻¹. In the region 3000-2809 cm⁻¹, bands of CH vibrations of aliphatic fatty acid chains were found. Moderately intense bands at 1740 and 1235 cm⁻¹ are typical for the presence of ester groups (valence vibrations C=O and C-O). The intense band at 1181 cm⁻¹ is due to the presence of ether bonds. This type of commercial binder is excellent for quick-drying primers and topcoats and has very good adhesion and chemical resistance. This type of binder is recommended by the manufacturer for the preparation of highly pigmented zinc anti-corrosion coatings.

Table 1. Specification of the tested epoxy ester binder

	Dry	Dry Content		Acid value	Color	Viscosity		
Binder	matter [%]	Oil [%]	EP-resin [%]	[mg KOH.g ⁻¹]	Color [-]	[mPa.s ⁻¹]	Forms	
Epoxy ester resin	60	40	60	3.9	10	4,200	60 % in xylene	

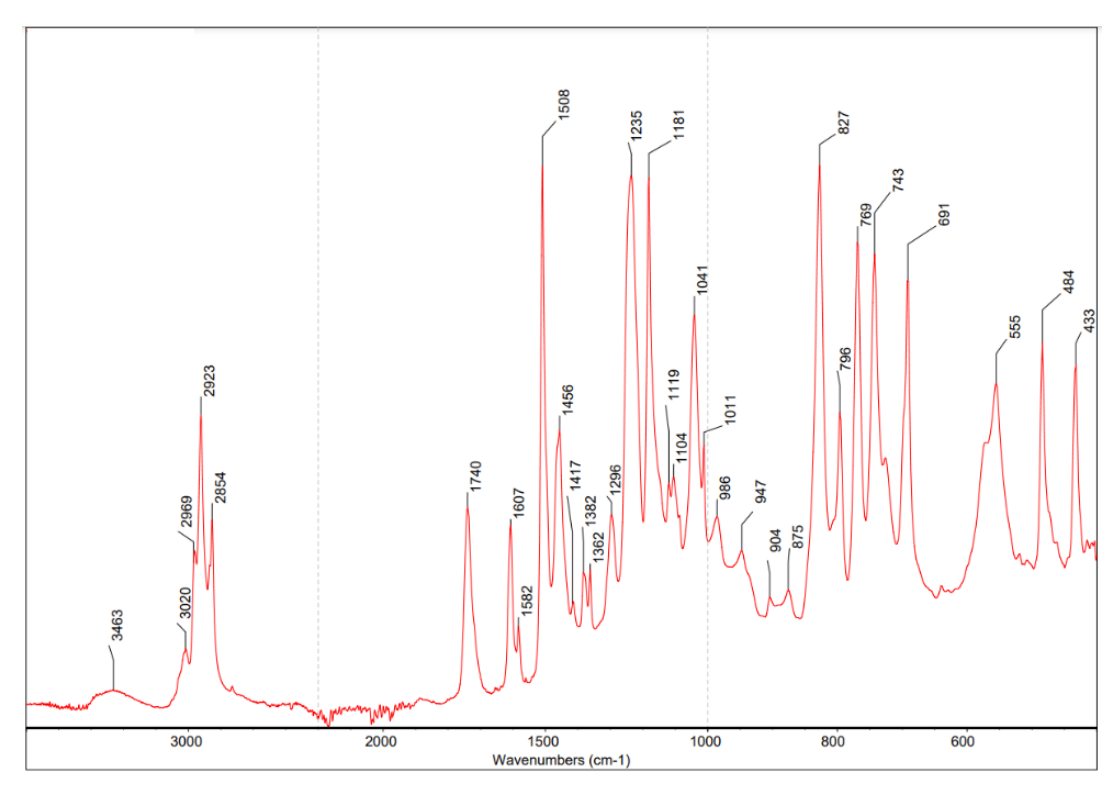


Figure 10. The FTIR spectrum of binder, which was used for the preparation of organic coating containing inorganic pigments.

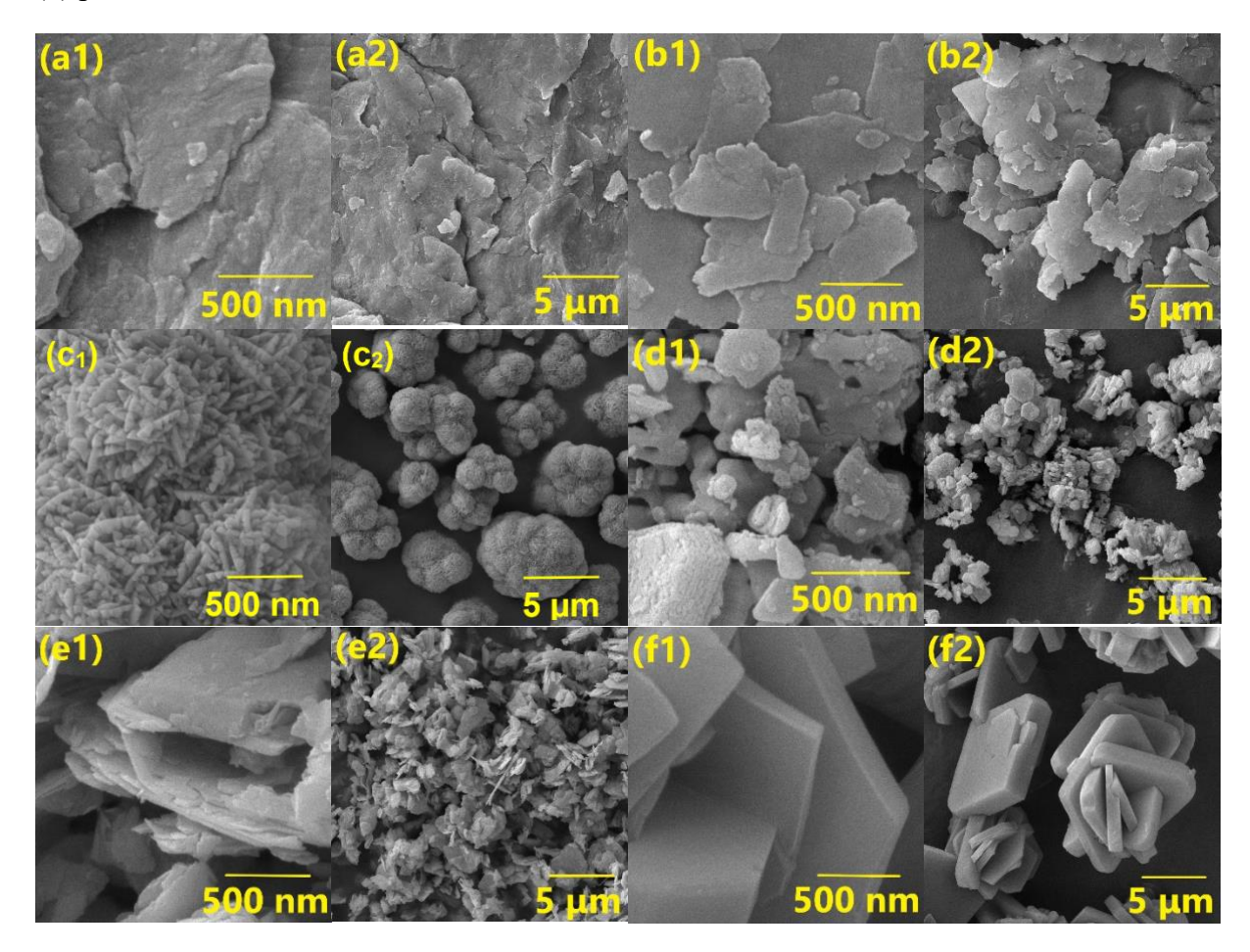
3.2. Characterization of the studied inorganic pigments

The eight types of inorganic pigments studied were subjected to measurements of the typical paint parameters, i.e., density and oil number, which are used to calculate the critical pigment volume concentration (CPVC) of each pigment. The results of the pigments studied are summarized in Table 2. The densities of the studied inorganic pigments ranged from 1.78 g.cm-3 (magnesium) to 7.1 g.cm⁻³ (zinc). The lowest oil absorption value (6.7 g/100g) was determined for metallic zinc dust, while the highest oil absorption value (48.1 g/100g) was determined for PANI-PTSA. The oil absorption values of other types of inorganic pigments ranged from 15.9 (ZnS) to 48.1 (MgO). The oil absorption parameter is significantly dependent on the surface area of the studied particles and thus also on the particle size [43], which was studied for individual types of inorganic pigments on the basis of micro-photographs taken by scanning electron microscopy (SEM). Based on the above-mentioned parameters (density and oil absorption), the CPVC parameter was calculated for individual types of inorganic pigments. The highest value of this parameter (66.0) was achieved specifically with metallic powdered zinc, while the lowest value of CPVC (36) was recorded with magnesium oxide pigment due to the high oil absorption recorded for this type of inorganic pigment.

Table 2. Characteristics of the studied inorganic pigments: density, oil absorption, and critical pigment volume concentration (CPVC)

Pigment	Density [g·cm ⁻³]	Oil absorption [g/100 g]	CPVC [-]
Mg	1.78 ±0.02	40.61 ±0.2	56.23
Al	2.45±0.02	40.9± 0.2	48.1
ZnS	4.05±0.02	15.9±0.2	59.2
MgO	3.01 ± 0.02	48.1±0.2	36
OP-Mg	1.38 ± 0.02	45.9±0.2	59
PANI-PTSA	1.41±0.02	74.3±0.2	46.7
MoS2	4.67±0.02	30.7±0.2	39.3
Zn	7.14 ± 0.02	6.7 ± 0.2	66.0

The representative SEM scans of inorganic pigments with different magnifications are shown in Figure 11. The measured SEM scans revealed that MoS2 (e) exhibit sheet-like structure (typical layered structure). The ZnS (c) formed polycrystalline spherical clusters with tetrahedral shape of primary nanoparticles (50-100 nm). The metallic Zn (h) particles possessed a predominantly spherical shape with 0.5-5 μ m in diameter. Metallic pigments Mg (a) and Al (b) possess flake like flat structure.



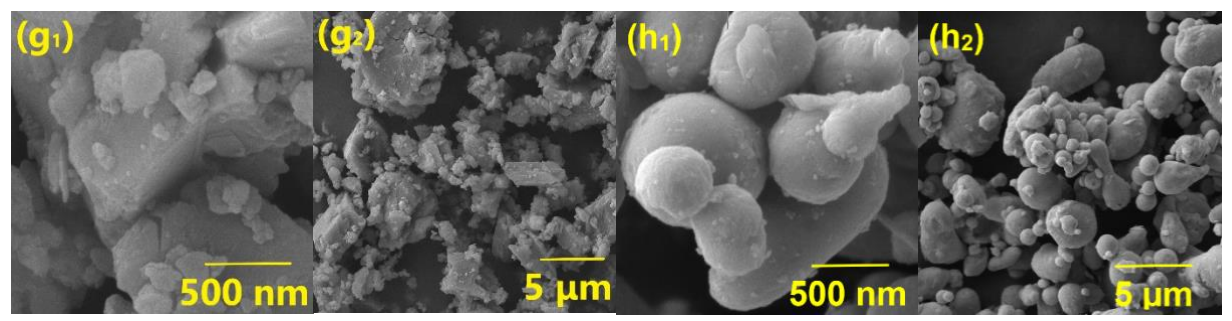


Figure 11. Scanning electron micrographs of the studied inorganic pigments: (a) Mg; (b) Al; (c) ZnS; (d) MgO; (e) MoS₂; (f) OP-Mg; (g) PANI-PTSA; (h) Zn.

3.3. Results of mechanical properties of the protective coatings

The mechanical properties of the investigated organic coatings, each incorporating different types of tested inorganic pigments (DFT = $90 \pm 10 \,\mu m$), were evaluated through seven distinct tests, as summarized in Table 3. As indicated in the table, the cupping test results were consistent across all coatings (>10 mm), with no visible damage observed when deformed up to 10 mm. Similarly, the impact test (100 cm) and bending test (5 mm) yielded comparable outcomes for all samples. Each coating successfully withstood the 100 cm impact and exhibited flexibility in the bending test, showing no signs of cracking or detachment when bent using a 5 mm mandrel.

The cross-cut adhesion test results for coatings containing different pigments were largely comparable. When the PANI-PTSA PVC content was maintained at a low level (0–3%), adhesion ratings ranged from 0 to 1. However, increasing the PANI-PTSA dosage led to reduced adhesion performance in all coatings, with ratings declining to 2. Pull-off adhesion results exhibited greater variability, ranging from 0.6 kN (lowest) to 1.1 kN (highest) across the samples. Notably, in the MEK resistance test, all coatings withstood more than 100 double rubs without visible degradation.

Hardness measurements revealed notable variations among the coatings. The highest hardness value (167 s) was observed in coatings containing MoS₂, while coatings with only zinc pigments exhibited the lowest value (139 s). Coatings with metallic pigments Mg and Al displayed comparable hardness, with Al-containing coatings showing slightly higher values. Similarly, coatings with organic pigments PANI-PTSA and Op-Mg exhibited nearly identical hardness, as did those with MgO and ZnS pigments, with ZnS providing marginally higher results. Furthermore, an increase in pigment PVC was associated with a noticeable improvement in coating hardness. Aditionally it was observed that hardness of coatings with zinc and other pigments is o=substantially higher that hardness of coatings with only zinc.

 Table 3. Results of mechanical properties of studied inorganic pigments

PANI- PTSA 1	Pigment	PVC [%]	Zn PVC [%]	PANI PTSA - PVC [%]	Cupping test (mm)	Impact test (cm)	Bending test (mm)	Pull off adhesion (kn)	Cross cut adhesion (2mm)	Hardness test (Persoz S)	MEK resistance
PTSA 5 45 -	DANI				>10			0.963	0		>100
Mg 1 45 - > >		3	45	-	>10	100		0.753	0	146	>100
Mg	FISA	5	45	-	>10	100	5	1.055	0	143	>100
Mig		1	45	-	>10	100	5	0.961	0	132	>100
1	Ma	3	45	-	>10	100	5	0.774	0	137	>100
1	Mg	1	45	1	>10	100	5	0.992	0	134	>100
1		3	45	1	>10	100	5	0.856	0	148	>100
Al		1	45	3	>10	100		0.704		145	>100
Al		3	45		>10	100		0.908		157	>100
Al											
Al 3 45 - >10 100 5 0.821 0 149 >100 1 45 1 >10 100 5 0.787 0 145 >100 3 45 1 >10 100 5 0.872 0 151 >100 1 45 3 >10 100 5 0.867 0 155 >100 3 45 3 >10 100 5 0.867 0 155 >100 3 45 3 >10 100 5 0.867 0 155 >100 3 45 5 >10 100 5 0.867 0 159 >100 1 45 5 >10 100 5 0.895 0 159 >100 1 45 5 >10 100 5 0.827 1 141 >100 ZnS 3 45 - >10 100 5 0.827 1 141 >100 ZnS 3 45 - >10 100 5 0.827 1 141 >100 ZnS 3 45 - >10 100 5 0.881 0 148 >100 5 45 - >10 100 5 0.881 0 148 >100 5 45 1 >10 100 5 0.695 0 152 >100 3 45 1 >10 100 5 0.695 0 152 >100 3 45 1 >10 100 5 0.668 0 153 >100 5 45 1 >10 100 5 0.668 0 153 >100 5 45 1 >10 100 5 1.031 0 153 >100 5 45 3 >10 100 5 1.052 0 151 >100 3 45 3 >10 100 5 1.052 0 151 >100 3 45 5 >10 100 5 0.958 1 148 >100 5 45 3 >10 100 5 1.052 0 151 >100 3 45 5 >10 100 5 1.045 2 149 >100 3 45 5 >10 100 5 1.045 2 149 >100 5 45 5 >10 100 5 1.045 2 152 >100 MoS2 3 45 - >10 100 5 1.045 2 152 >100											
Al		1	45	_	>10	100	5	0.711	0	143	>100
1	Al										
3 45 1 >10 100 5 0.872 0 151 >100 1 45 3 >10 100 5 0.867 0 155 >100 3 45 5 >10 100 5 0.895 0 159 >100 1 45 5 >10 100 5 0.895 0 159 >100 3 45 5 >10 100 5 0.895 0 159 >100 3 45 5 >10 100 5 0.827 1 141 >100 ZnS 3 45 - >10 100 5 0.827 1 141 >100 ZnS 3 45 - >10 100 5 0.581 0 148 >100 1 45 1 >10 100 5 0.581 0 148 >100 1 45 1 >10 100 5 0.695 0 152 >100 1 45 1 >10 100 5 0.695 0 152 >100 1 45 1 >10 100 5 0.695 0 152 >100 1 45 1 >10 100 5 0.668 0 153 >100 3 45 1 >10 100 5 1.031 0 153 >100 5 45 1 >10 100 5 1.052 0 151 >100 3 45 3 >10 100 5 1.052 0 151 >100 3 45 3 >10 100 5 0.958 1 148 >100 5 45 3 >10 100 5 0.958 1 148 >100 5 45 3 >10 100 5 1.052 0 151 >100 3 45 5 >10 100 5 1.045 2 149 >100 3 45 5 >10 100 5 1.045 2 149 >100 5 45 5 >10 100 5 1.045 2 149 >100 5 45 5 >10 100 5 1.045 2 149 >100 5 45 5 >10 100 5 1.045 2 152 >100 MoS ₂ 3 45 - >10 100 5 0.975 0 152 >100 1 45 1 >10 100 5 0.940 0 159 >100 1 45 1 >10 100 5 0.937 0 154 >100 1 45 3 >10 100 5 0.937 0 155 >100 1 45 3 >10 100 5 0.937 0 155 >100 1 45 3 >10 100 5 0.937 0 155 >100 1 45 3 >10 100 5 1.133 0 155 >100 1 45 3 >10 100 5 1.133 0 155 >100 1 45 3 >10 100 5 1.133 0 155 >100 1 45 3 >10 100 5 1.133 0 155 >100 3 45 3 >10 100 5 0.937 0 163 >100 5 45 1 >10 100 5 0.937 0 163 >100 5 45 1 >10 100 5 0.937 0 163 >100 5 45 3 >10 100 5 0.937 0 163 >100 5 45 3 >10 100 5 0.937 0 163 >100 5 45 3 >10 100 5 0.937 0 163 >100 5 45 3 >10 100 5 0.937 0 163 >100 5 45 5 >10 100 5 0.937 0 163 >100 5 45 5 >100 100 5 0.937 0 163 >100 5 45 5 >100 100 5 0.937 0 163 >100 5 45 5 >100 100 5 0.937 0 163 >100 5 45 5 >100 100 5 0.937 0 163 >100 5 45 5 >10 100 5 0.937 0 163 >100 5 45 5 >100 100 5 0.937 0 163 >100 5 45 5 >100 100 5 0.937 0 163 >100 5 45 5 >100 100 5 0.937 0 163 >100 5 45 5 >100 100 5 0.937 0 163 >100 5 45 5 >100 100 5 0.937 0 163 >100 5 45 5 >100 100 5 0.937 0 163 >100 5 45 5 >100 100 5 0.937 0 163 >100 5 45 5 >100 100 5 0.937 0 163 >100 5 45 5 >100 100 5 0.937 0 163 >100 5 45 5 >100 100 5 0.937 0 163 >100 5 45 5 >100 100 5 0.937 0 163 >100 5 45 5 >100 100 5 0.937 0 163 >100 5 45											
1											
3											
1											
ZnS 3 45 5 >10 100 5 0.827 1 141 >100 ZnS 3 45 - >10 100 5 0.581 0 144 >100 5 45 - >10 100 5 0.581 0 148 >100 5 45 - >10 100 5 0.695 0 152 >100 1 45 1 >10 100 5 1.090 0 147 >100 3 45 1 >10 100 5 0.668 0 153 >100 5 45 1 >10 100 5 1.031 0 153 >100 1 45 3 >10 100 5 1.052 0 151 >100 1 45 3 >10 100 5 1.052 0 151 >100 3 45 3 >10 100 5 0.958 1 148 >100 5 45 3 >10 100 5 1.175 1 158 >100 5 45 3 >10 100 5 1.045 2 149 >100 3 45 5 >10 100 5 1.045 2 149 >100 5 45 5 >10 100 5 1.073 2 146 >100 5 45 5 >10 100 5 1.175 0 155 >100 5 45 5 >10 100 5 1.045 2 152 >100 MoS ₂ 3 45 - >10 100 5 1.045 2 152 >100 1 45 1 >10 100 5 1.073 2 146 >100 MoS ₂ 3 45 - >10 100 5 1.189 0 155 >100 5 45 1 >10 100 5 1.137 0 154 >100 3 45 1 >10 100 5 1.137 0 154 >100 3 45 1 >10 100 5 1.137 0 154 >100 5 45 1 >10 100 5 1.036 0 155 >100 5 45 1 >10 100 5 1.036 0 155 >100 5 45 1 >10 100 5 1.036 0 155 >100 5 45 1 >10 100 5 1.036 0 155 >100 5 45 1 >10 100 5 1.036 0 155 >100 5 45 3 >10 100 5 1.133 0 155 >100 5 45 3 >10 100 5 1.133 0 155 >100 5 45 3 >10 100 5 1.207 1 158 >100 5 45 3 >10 100 5 0.937 0 163 >100 1 45 5 >10 100 5 0.937 0 163 >100 1 45 5 >10 100 5 0.937 0 163 >100 5 45 3 >10 100 5 0.937 0 163 >100 1 45 5 >10 100 5 0.937 0 163 >100 5 45 3 >10 100 5 0.937 0 163 >100 5 45 3 >10 100 5 0.937 0 163 >100 5 45 3 >10 100 5 0.937 0 163 >100 5 45 5 >10 100 5 0.937 0 163 >100 5 45 5 >10 100 5 0.937 0 163 >100 5 45 5 >10 100 5 0.937 0 163 >100 5 45 5 >10 100 5 0.937 0 163 >100 5 45 5 >10 100 5 0.937 0 155 >100 5 45 5 >10 100 5 0.937 0 155 >100 5 45 5 >10 100 5 0.937 0 155 >100 5 45 5 >10 100 5 0.937 0 155 >100 5 45 5 >10 100 5 0.937 0 155 >100 5 45 5 >10 100 5 0.937 0 155 >100 5 45 5 >10 100 5 0.937 0 155 >100 5 45 5 >10 100 5 0.937 0 155 >100 5 45 5 >10 100 5 0.937 0 155 >100 5 45 5 >10 100 5 0.937 0 155 >100 5 45 5 >10 100 5 0.937 0 155 >100 5 45 5 >10 100 5 0.937 0 155 >100 5 45 5 >10 100 5 0.937 0 151 >100											
ZnS 3 45 - >10 100 5 0.581 0 144 >100 5 45 - >10 100 5 0.581 0 148 >100 5 45 - >10 100 5 0.695 0 152 >100 1 45 1 >10 100 5 1.090 0 147 >100 3 45 1 >10 100 5 0.668 0 153 >100 5 45 1 >10 100 5 1.031 0 153 >100 1 45 3 >10 100 5 1.052 0 151 >100 3 45 3 >10 100 5 0.958 1 148 >100 5 45 3 >10 100 5 0.958 1 148 >100 5 45 3 >10 100 5 1.052 0 151 >100 3 45 5 >10 100 5 1.075 1 158 >100 1 45 5 >10 100 5 1.045 2 149 >100 5 45 5 >10 100 5 1.045 2 149 >100 5 45 5 >10 100 5 1.073 2 146 >100 MoS ₂ 3 45 - >10 100 5 1.073 2 146 >100 1 45 1 >10 100 5 1.137 0 155 >100 1 45 1 >10 100 5 1.137 0 155 >100 1 45 1 >10 100 5 1.137 0 155 >100 3 45 1 >10 100 5 1.137 0 155 >100 5 45 1 >10 100 5 1.137 0 154 >100 3 45 1 >10 100 5 1.036 0 155 >100 5 45 1 >10 100 5 1.036 0 155 >100 5 45 1 >10 100 5 1.036 0 155 >100 5 45 1 >10 100 5 1.33 0 155 >100 5 45 3 >10 100 5 1.33 0 155 >100 5 45 3 >10 100 5 1.33 0 155 >100 5 45 3 >10 100 5 1.33 0 155 >100 5 45 3 >10 100 5 1.33 0 155 >100 5 45 3 >10 100 5 1.33 0 155 >100 1 45 3 >10 100 5 1.33 0 155 >100 3 45 5 >10 100 5 1.33 0 155 >100 5 45 3 >10 100 5 1.33 0 155 >100 5 45 3 >10 100 5 0.937 0 163 >100 1 45 5 >10 100 5 0.937 0 163 >100 1 45 5 >10 100 5 0.937 0 163 >100 1 45 5 >10 100 5 0.937 0 163 >100 1 45 5 >10 100 5 0.937 0 163 >100 1 45 5 >10 100 5 0.937 0 163 >100 1 45 5 >10 100 5 0.937 0 163 >100 1 45 5 >10 100 5 0.937 0 163 >100 1 45 5 >10 100 5 0.937 0 163 >100 1 45 5 >10 100 5 0.937 0 163 >100 1 45 5 >10 100 5 0.937 0 163 >100 1 45 5 >10 100 5 0.937 0 163 >100 1 45 5 >10 100 5 0.937 0 163 >100 1 45 5 >10 100 5 0.939 2 155 >100 5 45 5 >10 100 5 0.939 2 155 >100 5 45 5 >10 100 5 0.939 2 155 >100 5 45 5 >10 100 5 0.999 2 153 >100 5 45 5 >10 100 5 0.999 2 153 >100 5 45 5 >10 100 5 0.999 2 153 >100 5 45 5 >10 100 5 0.999 2 153 >100											
ZnS 3 45 - >10 100 5 0.581 0 148 >100 5 45 - >10 100 5 0.695 0 152 >100 1 45 1 >10 100 5 0.695 0 152 >100 1 45 1 >10 100 5 0.695 0 152 >100 1 45 1 >10 100 5 0.668 0 153 >100 5 45 1 >10 100 5 1.031 0 153 >100 1 45 3 >100 1 45 3 >10 100 5 1.031 0 153 >100 1 45 3 >10 100 5 0.958 1 148 >100 1 1 45 3 >10 100 5 0.958 1 148 >100 1 45 5 >10 100 5 1.045 2 149 >100 1 45 5 >10 100 5 1.045 2 149 >100 1 45 5 >10 100 5 1.045 2 149 >100 1 1 45 5 >10 100 5 1.045 2 149 >100 1 1 45 5 >10 100 5 1.045 2 149 >100 1 1 45 5 >10 100 5 1.045 2 152 >100 1 1 45 1 >10 100 5 1.045 2 1 1 >10 100 1 1 1 1 1 1 1 1 1 1 1 1 1 1											
5 45 - >10 100 5 0.695 0 152 >100 1 45 1 >10 100 5 1.090 0 147 >100 3 45 1 >10 100 5 0.668 0 153 >100 5 45 1 >10 100 5 1.031 0 153 >100 1 45 3 >10 100 5 1.031 0 153 >100 1 45 3 >10 100 5 1.052 0 151 >100 3 45 3 >10 100 5 0.958 1 148 >100 5 45 3 >10 100 5 1.045 2 149 >100 1 45 5 >10 100 5 1.045 2 149 >100 3 45 5 >10 100 5 1.045 2 152 >100	- ~										
$\begin{array}{cccccccccccccccccccccccccccccccccccc$	ZnS			-							
3 45 1 >10 100 5 0.668 0 153 >100 5 45 1 >10 100 5 1.031 0 153 >100 1 45 3 >10 100 5 1.052 0 151 >100 3 45 3 >10 100 5 0.958 1 148 >100 5 45 3 >10 100 5 1.175 1 158 >100 1 45 5 >10 100 5 1.045 2 149 >100 3 45 5 >10 100 5 1.045 2 152 >100 5 45 5 >10 100 5 1.073 2 146 >100 5 45 5 >10 100 5 1.073 2 146 >100 MoS ₂ 3 45 - >10 100 5 1.189 0 155 >100 5 45 - >10 100 5 1.189 0 155 >100 5 45 - >10 100 5 1.137 0 154 >100 1 45 1 >10 100 5 1.37 0 154 >100 1 45 1 >10 100 5 1.37 0 154 >100 3 45 1 >10 100 5 1.37 0 154 >100 5 45 1 >10 100 5 1.33 0 155 >100 5 45 1 >10 100 5 0.937 0 163 >100 1 45 1 >10 100 5 0.937 0 163 >100 1 45 3 >10 100 5 1.133 0 155 >100 5 45 3 >10 100 5 1.133 0 155 >100 5 45 1 >10 100 5 0.937 0 163 >100 1 45 3 >10 100 5 1.133 0 155 >100 5 45 3 >10 100 5 1.33 0 155 >100 5 45 3 >10 100 5 0.937 0 163 >100 1 45 3 >10 100 5 0.937 0 163 >100 1 45 3 >10 100 5 0.937 0 163 >100 1 45 3 >10 100 5 0.937 0 163 >100 1 45 5 5 >10 100 5 0.937 0 163 >100 1 45 5 5 >10 100 5 0.937 0 163 >100 1 45 5 5 >10 100 5 0.937 0 163 >100 1 45 5 5 >10 100 5 0.937 0 163 >100 1 45 5 5 >10 100 5 0.937 0 163 >100 1 45 5 5 >10 100 5 0.937 0 163 >100 1 45 5 5 >10 100 5 0.937 0 163 >100 5 45 3 >10 100 5 0.937 0 163 >100 5 45 3 >10 100 5 0.937 0 163 >100 5 45 5 5 >10 100 5 0.937 0 163 >100 5 45 5 >10 100 5 0.937 0 163 >100 5 45 5 >10 100 5 0.937 0 163 >100 6 5 45 5 >10 100 5 0.937 0 163 >100 6 5 45 5 >10 100 5 0.939 2 153 >100 6 5 45 5 >10 100 5 0.939 2 153 >100 6 5 45 5 >10 100 5 0.939 2 155 >100 6 5 45 5 >10 100 5 0.999 2 153 >100 6 5 45 5 >10 100 5 0.995 2 162 >100											
5 45 1 >10 100 5 1.031 0 153 >100 1 45 3 >10 100 5 1.052 0 151 >100 3 45 3 >10 100 5 0.958 1 148 >100 5 45 3 >10 100 5 1.175 1 158 >100 1 45 5 >10 100 5 1.045 2 149 >100 3 45 5 >10 100 5 1.045 2 149 >100 5 45 5 >10 100 5 1.045 2 152 >100 5 45 5 >10 100 5 1.045 2 152 >100 5 45 5 >10 100 5 1.073 2 146 >100 MoS2 3 45 - >10 100 5 1.189 0 155 >100											
$\begin{array}{cccccccccccccccccccccccccccccccccccc$											
$\begin{array}{cccccccccccccccccccccccccccccccccccc$											
$\begin{array}{c ccccccccccccccccccccccccccccccccccc$											
$\begin{array}{c ccccccccccccccccccccccccccccccccccc$											
$\begin{array}{c ccccccccccccccccccccccccccccccccccc$		5									
$ \begin{array}{c ccccccccccccccccccccccccccccccccccc$											
$ \begin{array}{cccccccccccccccccccccccccccccccccccc$											
MoS_2 3 45 - >10 100 5 1.189 0 155 >100 5 45 - >10 100 5 0.940 0 159 >100 1 45 1 >10 100 5 1.137 0 154 >100 3 45 1 >10 100 5 1.036 0 155 >100 5 45 1 >10 100 5 0.937 0 163 >100 1 45 3 >10 100 5 1.133 0 155 >100 3 45 3 >10 100 5 1.207 1 158 >100 5 45 3 >10 100 5 0.763 2 167 >100 5 45 3 >10 100 5 0.897 2 153 >100 3 45 5 >10 100 5 0.897 2 <td< th=""><td></td><td>5</td><td>45</td><td>5</td><td>>10</td><td>100</td><td>5</td><td>1.073</td><td>2</td><td>146</td><td>>100</td></td<>		5	45	5	>10	100	5	1.073	2	146	>100
5 45 - >10 100 5 0.940 0 159 >100 1 45 1 >10 100 5 1.137 0 154 >100 3 45 1 >10 100 5 1.036 0 155 >100 5 45 1 >10 100 5 0.937 0 163 >100 1 45 3 >10 100 5 1.133 0 155 >100 3 45 3 >10 100 5 1.207 1 158 >100 5 45 3 >10 100 5 0.763 2 167 >100 1 45 5 >10 100 5 0.897 2 153 >100 3 45 5 >10 100 5 0.897 2 155 >100 5 45 5 >10 100 5 0.795 2 162 >100 </th <td></td> <td></td> <td></td> <td>-</td> <td>>10</td> <td></td> <td></td> <td>0.975</td> <td>0</td> <td>152</td> <td>>100</td>				-	>10			0.975	0	152	>100
1 45 1 >10 100 5 1.137 0 154 >100 3 45 1 >10 100 5 1.036 0 155 >100 5 45 1 >10 100 5 0.937 0 163 >100 1 45 3 >10 100 5 1.133 0 155 >100 3 45 3 >10 100 5 1.207 1 158 >100 5 45 3 >10 100 5 0.763 2 167 >100 1 45 5 >10 100 5 0.929 2 153 >100 3 45 5 >10 100 5 0.897 2 155 >100 5 45 5 >10 100 5 0.795 2 162 >100	MoS_2			-				1.189	0		>100
3 45 1 >10 100 5 1.036 0 155 >100 5 45 1 >10 100 5 0.937 0 163 >100 1 45 3 >10 100 5 1.133 0 155 >100 3 45 3 >10 100 5 1.207 1 158 >100 5 45 3 >10 100 5 0.763 2 167 >100 1 45 5 >10 100 5 0.929 2 153 >100 3 45 5 >10 100 5 0.897 2 155 >100 5 45 5 >10 100 5 0.795 2 162 >100		5	45	-	>10	100		0.940	0	159	>100
5 45 1 >10 100 5 0.937 0 163 >100 1 45 3 >10 100 5 1.133 0 155 >100 3 45 3 >10 100 5 1.207 1 158 >100 5 45 3 >10 100 5 0.763 2 167 >100 1 45 5 >10 100 5 0.929 2 153 >100 3 45 5 >10 100 5 0.897 2 155 >100 5 45 5 >10 100 5 0.795 2 162 >100				1	>10		5	1.137	0		>100
1 45 3 >10 100 5 1.133 0 155 >100 3 45 3 >10 100 5 1.207 1 158 >100 5 45 3 >10 100 5 0.763 2 167 >100 1 45 5 >10 100 5 0.929 2 153 >100 3 45 5 >10 100 5 0.897 2 155 >100 5 45 5 >10 100 5 0.795 2 162 >100			45	1	>10	100		1.036	0	155	>100
1 45 3 >10 100 5 1.133 0 155 >100 3 45 3 >10 100 5 1.207 1 158 >100 5 45 3 >10 100 5 0.763 2 167 >100 1 45 5 >10 100 5 0.929 2 153 >100 3 45 5 >10 100 5 0.897 2 155 >100 5 45 5 >10 100 5 0.795 2 162 >100		5	45	1	>10	100	5	0.937	0	163	>100
3 45 3 >10 100 5 1.207 1 158 >100 5 45 3 >10 100 5 0.763 2 167 >100 1 45 5 >10 100 5 0.929 2 153 >100 3 45 5 >10 100 5 0.897 2 155 >100 5 45 5 >10 100 5 0.795 2 162 >100		1	45	3	>10	100		1.133		155	>100
5 45 3 >10 100 5 0.763 2 167 >100 1 45 5 >10 100 5 0.929 2 153 >100 3 45 5 >10 100 5 0.897 2 155 >100 5 45 5 >10 100 5 0.795 2 162 >100											
1 45 5 >10 100 5 0.929 2 153 >100 3 45 5 >10 100 5 0.897 2 155 >100 5 45 5 >10 100 5 0.795 2 162 >100 1 45 >10 100 5 0.830 0 141 >100											
3 45 5 >10 100 5 0.897 2 155 >100 5 45 5 >10 100 5 0.795 2 162 >100									2		
5 45 5 >10 100 5 0.795 2 162 >100 1 45 >10 100 5 0.830 0 141 >100		3	45					0.897	2		
1 45 - >10 100 5 0.830 0 141 >100			45								
On 1 15 10 100 5 01050 0 111 100	OP	1	45	_	>10	100	5	0.830	0	141	>100
OP- 3 45 >10 100 5 0.610 0 145 >100				-							
\mathbf{Mg} 1 45 1 >10 100 5 1.116 0 140 >100	Mg			1							
3 45 1 >10 100 5 0.577 0 144 >100							5				
1 45 3 >10 100 5 0.827 1 143 >100											
3 45 3 >10 100 5 0.977 1 147 >100											
1 45 5 >10 100 5 1.097 1 145 >100											

	3	45	5	>10	100	5	1.192	0	148	>100
MgO	1 3	45 45	-	>10 >10	100 100	5 5	0.756 0.964	0	138 141	>100 >100
50	1	45	1	>10	100	5	1.096	ő	141	>100
	3	45	1	>10	100	5	1.090	1	147	>100
	1	45	3	>10	100	5	1.278	2	143	>100
	3	45	3	>10	100	5	1.087	0	147	>100
	1	45	5	>10	100	5	1.084	1	144	>100
	3	45	5	>10	100	5	1.088	1	145	>100
Zn	-	45		>10	100	5	0.887	1	139	>100

3.4. Anti-corrosion efficiency of pigmented epoxy ester coatings in an atmosphere containing salt electrolyte

The studied organic coatings with DFT = 90 ± 5 µm were exposed in a salt electrolyte atmosphere for 960 h. A photograph of the selected organic coating after 960 hours of exposure in an atmosphere containing salt electrolyte and steel panels after removing the organic coatings are shown in **Figure 12**, **13 and 14**. During the exposure, the degree of blistering outside and in the area of the test section was evaluated, and after the exposure of each organic coating, the degree of adhesion was determined. Subsequently, the organic coating was removed, and the corrosion manifestations on the steel panel were evaluated. The results of the individual parameters evaluated after 960 h exposure are shown in **Table 4**.

Based on the results of the individual organic coatings studied after 960 h of exposure in this type of corrosive atmosphere, following results can be concluded.

For coatings containing zinc (PVC 45), blistering of small size but high density (8D) was observed across the coating film. In contrast, blistering at the cut was larger in size (6MD). Corrosion of the substrate was severe, with more than 50% of the area covered by red rust, and corrosion penetration at the cut reaching up to 4 mm. These coatings were considered as the baseline for comparison with other formulations. (Figure 12)

Coatings incorporating zinc along with metallic pigments such as magnesium and aluminum exhibited improved performance compared to zinc-only systems. The addition of magnesium metallic pigment (PVC 3%) to zinc (PVC 45%) resulted in medium-density blistering on the surface (6M) and at the cut (4M). Corrosion resistance was markedly enhanced, with almost no corrosion on the substrate and only 2 mm of penetration at the cut. Similarly, the incorporation of PANI-PTSA (PVC 1%) into zinc–magnesium coatings (zinc 45%, magnesium 3%) produced comparable results. However, increasing the dosage of PANI-PTSA

led to a reduction in corrosion resistance. Coatings formulated with zinc in combination with aluminum metallic pigments also demonstrated superior performance compared to zinc-only coatings. Incorporating aluminum (PVC 3%) into a zinc matrix (PVC 45%) resulted in high-density blistering on the surface (4D) and almost no blisters at the cut area. Corrosion protection was greatly improved, with negligible substrate corrosion and only 2 mm penetration at the cut. Likewise, the addition of PANI-PTSA (PVC 1%) to zinc-aluminum coatings (zinc 45%, aluminum 3%) yielded different outcome with higher surface corrosion (10%). However, higher concentrations of PANI-PTSA were found to diminish the corrosion resistance of the coatings. When comparing the performance of aluminum and magnesium as metallic pigments, magnesium demonstrated superior corrosion resistance when combined with zinc. This trend is clearly reflected in the experimental results. (Figure 12)

Incorporation of zinc and inorganic pigments, such as ZnS and MgO, enhances the overall performance of zinc-rich coatings. Among these, MgO demonstrated superior results; when incorporated at (PVC 3%) into zinc-rich coatings and subjected to 960 hours of salt spray testing, the coating exhibited (6D) blistering at the cut and (6MD) blistering across the surface. After film removal, only (3%) of the substrate showed corrosion, with corrosion at the cut spreading 1–1.5 mm. Similarly, coatings containing (PVC 3%) of ZnS exhibited (2M) blistering at the cut and (6M) blistering across the surface. Following film removal, 16% of the substrate area was corroded, with 1–1.5 mm corrosion spreading at the cut. In contrast, MoS₂ displayed poor performance, as surface corrosion reached (50%). Notably, the addition of just (PVC 1%) of PANI-PTSA to all these coatings significantly improved their performance, reducing corrosion to nearly 1%. (Figure 13)

Zinc coatings containing the organic anticorrosion pigment OP-Mg (3% PVC) exhibited excellent performance after 960 hours of salt spray testing. Blistering at both the cut and the coating surface was rated (4D). Following film removal, only 3% of the substrate surface showed corrosion, with corrosion at the cut limited to a 0.5 mm spread. However, the incorporation of PANI-PTSA into these coatings did not result in any further improvement. (Figure 14)

Table 4. Results of the corrosion test performed in an atmosphere of NaCl + $(NH_4)_2SO_4$ of the studied organic coatings containing inorganic pigment (PVC = 3, 5 and 10 %) and zinc (PVC/CPVC = 0.60) after 960 hours of exposure, DFT = $90\pm5~\mu m$

Pigment	PVC [%]	Zn PVC [%]	PANI PTSA - PVC	Blistering	Corrosion
---------	------------	---------------	-----------------------	------------	-----------

			[%]	In the cut [dg.]	On the film area [dg.]	Metal base [%]	In the cut [mm]
DANII	1	45	-	6D	6D	50	3.5-4
PANI- PTSA	3	45	-	2D	2D	50	3.5-4
1 15A	5	45	-	2D	2MD	33	3.5-4
	1	45	-	4D	6D	33	3.5-4
3.6	3	45	-	4M	6M	-	2-2.5
Mg	1	45	1	6MD	6D	33	2.5-3
	3	45	1	2D	6D	3	2-2.5
	1	45	3	4M	4D	16	3.5-4
	3	45	3	2D	2MD	33	1.5-2
	1	45	5	2MD	2M	50	2-2.5
	3	45	5	2M	6M	16	1.5-2
	1	45	-	4D	8F	3	1.5-2
	3	45	_	4D	-	10	2-2.5
Al	1	45	1	4D	- 6MD	10	1.5-2
	3	45	1	4D	6D	16	2-2.5
	1	45	3	4D 2D	4D	50	3.5-4
	3	45	3	6D	6MD	33	1-1.5
	1	45	5	2D	4D	50	3.5-4
	3	45	5	2D 2M	4D 4M	30 16	3.5 -4 1.5-2
		45					
77. 0	1	45 45	-	2M	-	10	1.5-2
ZnS	3		=	2M	6M	16	1-1.5
	5	45	-	2MD	8F	10	1-1.5
	1	45	1	8M	8M	3	0.5-1
	3	45	1	2D	6MD	3	0.5-1
	5	45	1	6D	8F	1	0.5-1
	1	45	3	2D	6D	33	1-1.5
	3	45	3	2D	6D	50	1.5-2
	5	45	3	4D	6D	16	0.5-1
	1	45	5	4M	4M	10	0.5-1
	3	45	5	4D	4MD	16	0.5-1
	5	45	5	2D	6MD	50	1-1.5
	1	45	-	4F	-	50	2-2.5
MoS_2	3	45	-	2D	2M	50	1-1.5
	5	45	-	2D	2MD	50	1-1.5
	1	45	1	2D	2MD	50	2-2.5
	3	45	1	2D	4MD	3	1-1.5
	5	45	1	2D	2D	33	2-2.5
	1	45	3	2D	2D	10	2-2.5
	3	45	3	2D	2D	50	2-2.5
	5	45	3	2D	4D	10	2.5-3
	1	45	5	2D	4D	16	3.5-4
	3	45	5	2D	4D	16	2-2.5
	5	45	5	2D	4D	10	2-2.5
	1	45		4D	4D	50	1.5-2
OP-Mg	3	45	_	4D 4D	4D 4D	3	0.5-1
J1 -1/1g	1	45	1	2D	4D 8M	50	3.5-4
	3	45	1	2MD	4M	10	1.5-2
		45	3	21VID 4D			
	1				4D	1	0.5-1
	3	45	3	4D	4D	3	1-1.5

	1	45	5	2D	4D	16	2-2.5
	3	45	5	2M	4MD	3	2-2.5
	1	45	-	4D	6D	1	1-1.5
MgO	3	45	-	6D	6MD	3	1-1.5
	1	45	1	6D	6MD	1	0.5-1
	3	45	1	2D	4D	3	1.5-2
	1	45	3	4D	4D	3	1-1.5
	3	45	3	4D	4D	10	1-1.5
	1	45	5	4D	4MD	3	1-1.5
	3	45	5	2D	4D	3	1-1.5
Zn	PVC/CPV C = 0.45	45	-	6MD	8D	50	3.5-4

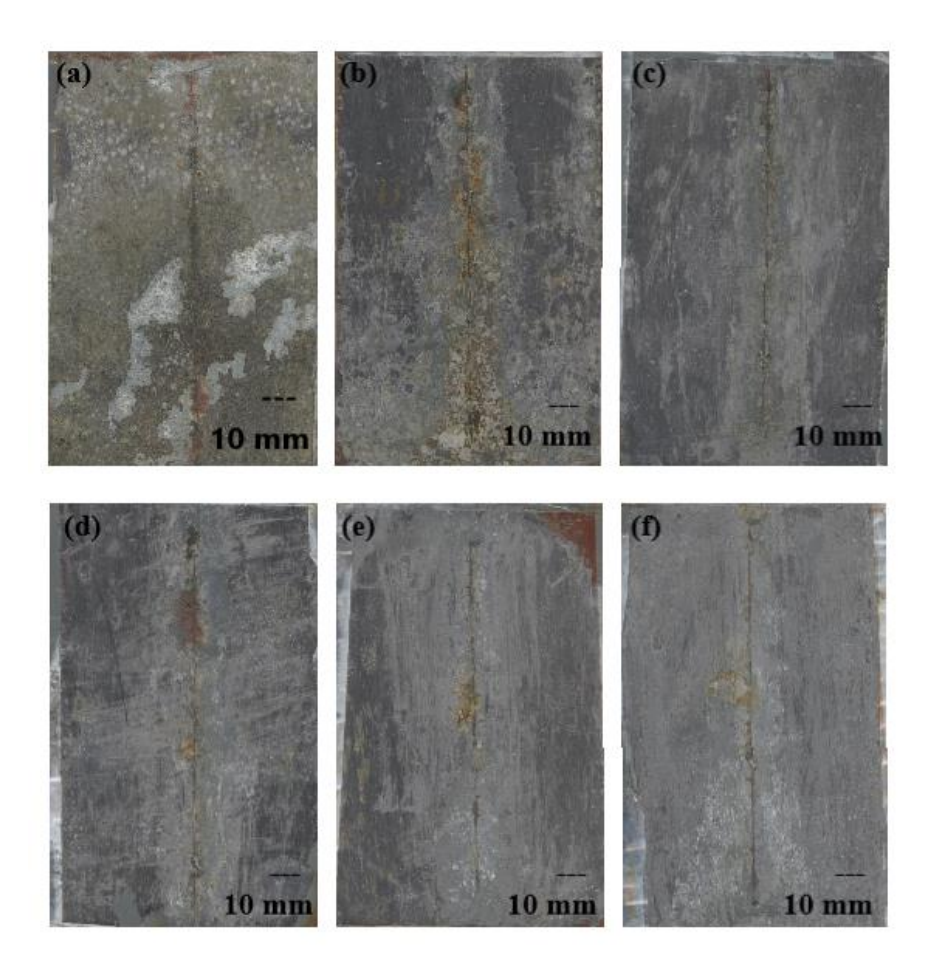


Figure 12. Organic coating after 960 hours of exposure in an atmosphere containing salt electrolyte: (a) with Zn at PVC = 45 %; (b) Zn PVC 45% with PANI-PTSA PVC 3 %; (c) Zn PVC 45% with Mg PVC 3% (d) Zn PVC 45% with Mg PVC 3% PANI-PTSA PVC 1%: (e) Zn PVC 45% with Al PVC 3%; (f) Zn PVC 45% with Al PVC 3% PANI-PTSA PVC 1%

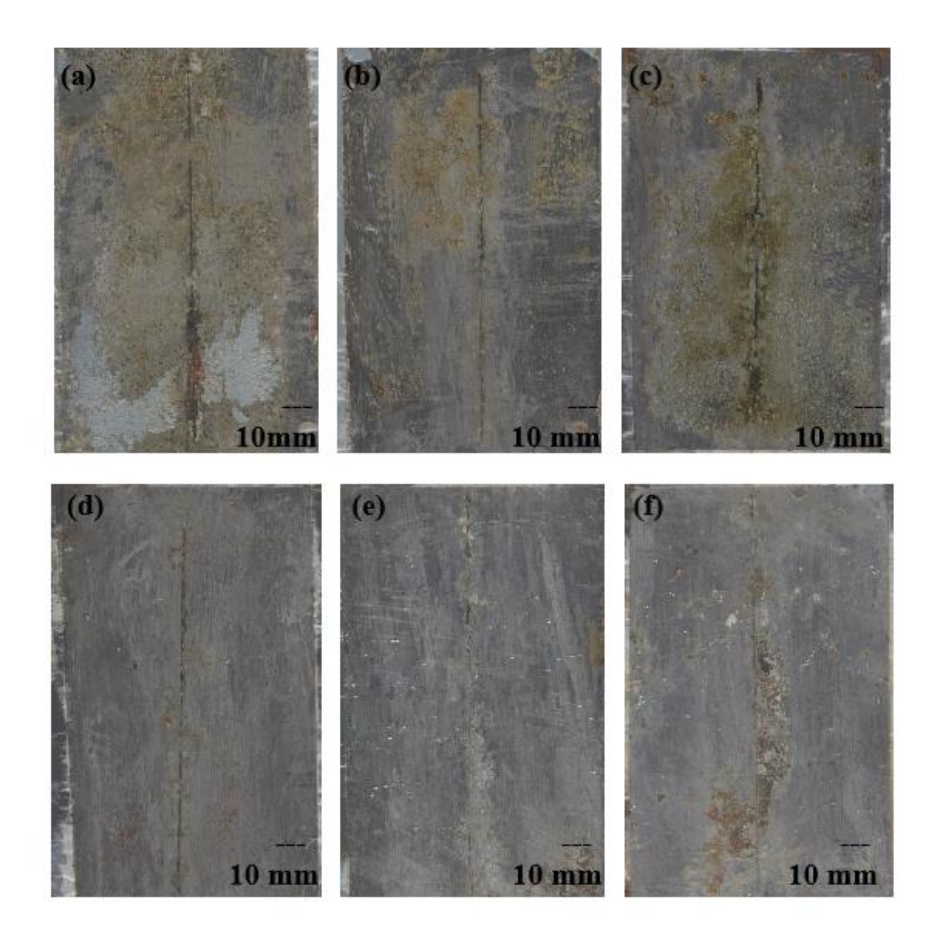


Figure 13. Organic coating after 960 hours of exposure in an atmosphere containing salt electrolyte: (a) Zn PVC = 45 % with ZnS PVC 3%; (b) Zn PVC 45% with ZnS PVC 3% PANI-PTSA PVC 3%; (c) Zn PVC 45% with MoS₂ PVC 3% (d) Zn PVC 45% with MoS₂ PVC 3% PANI-PTSA PVC 1%: (e) Zn PVC 45% with MgO PVC 3%; (f) Zn PVC 45% with MgO PVC 3% PANI-PTSA PVC 1%

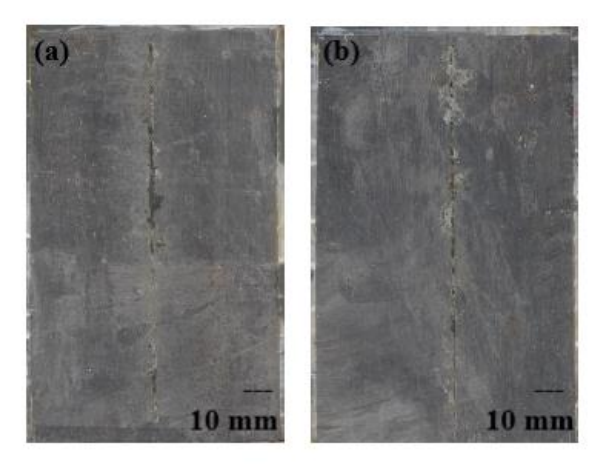


Figure 14. Organic coating after 960 hours of exposure in an atmosphere containing salt electrolyte: (a) Zn PVC = 45 % with OP-Mg 3%; (b) Zn PVC 45% with OP-Mg PVC 3% PANI-PTSA PVC 1 %

4. Conclusion

The present study demonstrates that the incorporation of metallic, inorganic, and organic anticorrosive pigments in epoxy ester—based zinc rich coatings significantly enhances their protective performance. Metallic pigments such as magnesium (Mg) and aluminum (Al) contributed to improved corrosion resistance primarily through their sacrificial protection mechanism, where these active metals preferentially oxidize, thereby protecting the underlying steel substrate. In addition, inorganic pigments like magnesium oxide (MgO) enhanced barrier properties by forming a compact and adherent oxide layer that reduces the permeability of corrosive species such as water and oxygen.

Among the various formulations tested, coatings containing small quantities of MgO combined with PANI-PTSA (polyaniline p-toluenesulfonic acid) exhibited the best overall corrosion resistance, indicating a synergistic effect between the inorganic oxide and conductive polymer pigment. Organic anticorrosive pigments, particularly OP-Mg, also showed promising performance due to their passive barrier effect and capability to stabilize the coating matrix. The inclusion of PANI-PTSA further improved the electrochemical stability of the coatings by facilitating charge transfer and forming a redox-active layer that delays corrosion initiation.

Conversely, MoS₂-containing systems performed poorly in comparison, likely due to their lubricating nature, which can reduce coating adhesion and disrupt protective film integrity. Overall, this research confirms that the combination of MgO and PANI-PTSA offers an optimal balance of active and passive corrosion protection mechanisms, making it a highly effective pigment system for advanced anticorrosive coating formulations.

Acknowledgment

The authors are thankful for financial support from the Ministry of Education, Youth and Sports of the Czech Republic (grant LM2023037).

References

- [1] Zhang, Y., Su, J., Xiao, X., Wang. N., Meng, G., Gu, Li. Graphene-like two-dimensional nanosheets-based anticorrosive coatings: A review. *Journal of Materials Science & Technology*, **2022**, 129 (1), 139-162. doi.org/10.1016/j.jmst.2022.04.032
- [2] Stejskal J., Trchová M., Brodinová J., Kalenda P., Fedorová S., Prokeš J., Zemek J., Coating of zinc ferrite particles with a conducting polymer, polyaniline. *Journal of Colloid and Interface Science*, **2006**, 298 (1), 87-93. doi.org/10.1016/j.jcis.2005.12.034
- [3] Rostami, M., Rasouli, S., Ramezanzadeh, B., Askari, A., Electrochemical investigation of the properties of Co doped ZnO nanoparticle as a corrosion inhibitive pigment for modifying corrosion resistance of the epoxy coating, *Corrosion Science*, **20**14, 88, 387-399. doi.org/10.1016/j.corsci.2014.07.056
- [4] Nikravesh, B., Ramezanzadeh, B., Sarabi, A.A., Kasiriha, S.M., Evaluation of the corrosion resistance of an epoxy-polyamide coating containing different ratios of micaceous iron oxide/Al pigments, *Corrosion Science*, **2011**, 53(4),1592-1603. doi.org/10.1016/j.corsci.2011.01.045
- [5] Kalendová, A., Veselý, D., Kohl, M., Stejskal, J. Anticorrosion efficiency of zinc-filled epoxy coatings containing conducting polymers and pigments. *Progress in Organic Coatings*. **2015**, 78, 1-20. doi.org/10.1016/j.porgcoat.2014.10.009
- [6] Havlík, J., Kalendová, A., Veselý, D., Electrochemical, chemical and barrier action of zinc dust/anticorrosive pigments containing coatings. *Journal of Physics and Chemistry of Solids*, **2007**, 68 (5-6), 1101-1105. doi.org/10.1016/j.jpcs.2006.11.016
- [7] Hussain, A. K., Seetharamaiah, N., Pichumani, M., Chakra, Ch. S., Research progress in organic zinc rich primer coatings for cathodic protection of metals A comprehensive review. *Progress in Organic coatings*, **2021**, 153, 106040. doi.org/10.1016/j.porgcoat.2020.106040
- [8] Ahmadzadeh, M., Shahrabi, T., Izadi, M., Mohammadi, I., Hoseinieh, S. M., Barnoush, A., Calcareous scales deposited in the organic coating defects during artificial seawater cathodic protection: Effect of zinc cations. *Journal of Alloys and Compounds*, **2019**, 784 (5), 744-755. doi.org/10.1016/j.jallcom.2019.01.096
- [9] Feng, Y., Wang, L., Yang, Z., Ma, Q., He, D., Xu, K., Zhang, H., Zhang P., Sun, W., Liu, G., Effect of ZnO as corrosion product on corrosion behavior of zinc-iron corrosion protection systems, *Corrosion Science*, 2024, 227, 111802. doi.org/10.1016/j.corsci.2023.111802
- [10] Ma, Q., Wang, L., Sun, W., Yang, Z., Wang, S., Liu, G., Effect of chemical conversion induced by self-corrosion of zinc powders on enhancing corrosion protection performance of zinc-rich coatings, *Corrosion Science*, **2022**, 194, 109942. doi.org/10.1016/j.corsci.2021.109942
- [11] Arman, S.Y., Ramezanzadeh, B., Farghadani, S., Mehdipour, M., Rajabi, A., Application of the electrochemical noise to investigate the corrosion resistance of an epoxy zinc-rich coating loaded with lamellar aluminum and micaceous iron oxide particles, *Corrosion Science*, **2013**, 77, 118-127. doi.org/10.1016/j.corsci.2013.07.034
- [12] Müller, B., Oughourlian ,C., Schubert, M., Amphiphilic copolymers as corrosion inhibitors for zinc pigment, *Corrosion Science*, **2000**, 42(3), 577-584. doi.org/10.1016/S0010-938X(99)00093-1

- [13] Kalantar-zadeh, K., Ou, J. Z., Daeneke, T., Mitchell, A., Sasaki, T., Fuhrer, M. S. Two dimensional and layered transition metal oxides. *Applied materials today*, **2016**, 5, 73-89. doi.org/10.1016/j.apmt.2016.09.012
- [14] Wert, S., Iffelsberger, Ch., Novčić, K. A., Pumera, M., Corrosion of catalyst in high resolution: Layered transition metal dichalcogenides electrocatalyse water splitting and corrode during the process. *Journal of Catalysis*, **2022**, 416, 85-91. doi.org/10.1016/j.jcat.2022.10.023
- [15] Sinha, A., Dhanjai, Tan, B., Huang, Y., Thao, H., Dang, X., Chen, J., Jain, R., MoS₂ nanostructures for electrochemical sensing of multidisciplinary targets: A review. *TrAC Trends in Analytical Chemistry*, **2018**, 102, 75-90. doi.org/10.1016/j.trac.2018.01.008
- [16] Naguib, M., Gogotsi, Y., Synthesis of two-dimensional materials by selective extraction. *Accounts of Chemical Research.* **2015**, 48, 128-135. doi.org/10.1021/ar500346b
- [17] Mas-Ballesté, R., Gómez-Navarro, C., Gómez-Herrero, J., Zamora, F., 2D materials: To graphene and beyond. *Nanoscale*, **2011**, 3(1), 20-30. doi.org/10.1039/C0NR00323A
- [18] Sadanandan, A., Thomas, S. A., Khan, M. E., Alomar, M. S., Pallavolu, M. R., Cherusseri, J., A critical review on two-dimensional Ti₃C₂T_x MXenes for anti-corrosion coatings. *Progress in Organic Coatings*, **2023**, 183, 107757. doi.org/10.1016/j.porgcoat.2023.107757
- [19] Xia, Z., Liu, G., Dong, Y., Zhang, Y., Anticorrosive epoxy coatings based on polydopamine modified molybdenum disulfide. *Progress in Organic Coatings*, **2019**, 133, 154-160. doi.org/10.1016/j.porgcoat.2019.04.056
- [20] Lv, R., Robinson, J. A., Schaak, R. E., Sun, D., Sun, Y., Mallouk, T. E., Terrones, M., Transition Metal Dichalcogenides and Beyond: Synthesis, Properties, and Applications of Single- and Few-Layer Nanosheets. *Accounts of Chemical Research*, **2015**, 48, 56-64. doi.org/10.1021/ar5002846
- [21] Joswig, J. O., Lorenz, T., Wendumu, T. B., Gemming, S., Seifert, G., Optics, Mechanics, and Energetics of Two-Dimensional MoS₂ Nanostructures from a Theoretical Perspective. *Accounts of Chemical Research*, **2015**, 48, 48-55. doi.org/10.1021/ar500318p
- [22] Eksik, O., Gao, J., Shojaee, S. A., Thomas, A., Chow, Philippe, Bartolucci, S. F., Lucca, D. A., Karotkar, N., Epoxy Nanocomposites with Two-Dimensional Transition Metal Dichalcogenide Additives. *ACS Nano*, **2014**, 8 (5), 5282-5289. doi.org/10.1021/nn5014098
- [23] Tan, W., Zhao, W., Designing WS₂@Ti₃C₂T_x heterojunction nanofillers via electrostatic self-assembly for achieving long term corrosion resistance under AHP environment. *Materials Today Nano*, **2022**, 20, 100259. doi.org/10.1016/j.mtnano.2022.100259
- [24] Gnanaprakasam, P., Mangalaraja, R. V., Salvo, C., Microwave driven synthesis of tungsten sulfide nanosheets: An efficient electrocatalyst for oxygen reduction reaction. *Materials Science in Semiconductor Processing*, **2022**, 137, 106213. doi.org/10.1016/j.mssp.2021.106213
- [25] Rana, D. S., Thakur, N., Singh, D., Sonia, P., Molybdenum and tungsten disulfide based nanocomposites as chemical sensor: A review. *Materialstoday: Proceedings*, **2022**, 62(6), 2755-2761. doi.org/10.1016/j.matpr.2022.01.147
- [26] Joseph, A., Eapen, M. K., Mampillly, M. E., Sajith, V., Comparison of Corrosion Resistance Properties of Electrophoretically Deposited MoS₂ and WS₂ Nanosheets Coatings on Mild Steel. *Metallurgical and Materials Transactions A*, **2021**, 52, 3689-3693. doi.org/10.1007/s11661-021-06354-x
- [27] Hwnag, H. Y., Isawa, Y., Kawasaki, M., Keimer, B., Nagaosa, N., Tokura, Y., Emergent phenomena at oxide interfaces. *Nature Materials*, **2012**, 11, 103-113. doi.org/10.1038/nmat3223
- [28] R. Holm, Magnesium Compounds—A Review of the Current Market and Applications, Industrial Minerals, 2019.
- [29] J. Park & S. Lee, "Anticorrosive Properties of Magnesium Oxide-Based Coatings," *Surface and Coatings Technology*, Vol. 258, 2014, pp. 123–130.
- [30] A. S. Wypych, *Handbook of Fillers*, 4th ed., ChemTec Publishing, 2016.
- [31] Giudice, Carlos A.: Tecnología de pinturas y recubrimientos: componentes, formulación, manufactura y calidad/Carlos A. Giudice y Andrea M. Pereyra. 1a ed., Buenos Aires: Edutecne, **2009**. ISBN 978-987-25360-2-2.

- [32] Buxbaum, Gunter Industrial Inorganic Pigments/Edited by Gunter Buxbaum. 2nd completely rev. Weinheim; New York: Wiley-VCH, **1998**, ISBN: 3-527-28878-3.
- [33] Bierwagen, G. P., "Electrochemical Aspects of Paints and Coatings for Corrosion Protection," *Progress in Organic Coatings*, Vol. 28, Issue 1, 1996, pp. 43–48.
- [34] Sinko, J., "Progress in Corrosion Protection of Metallic Surfaces by Organic Coatings," *Progress in Organic Coatings*, Vol. 43, Issue 1-3, 2001, pp. 85–104.
- [35] Wicks, Z. W., Jones, F. N., & Pappas, S. P., *Organic Coatings: Science and Technology*, 3rd ed., Wiley-Interscience, 2007.
- [36] Verma, C., Haque, J., Quraishi, M.A., Ebenso, E.E., Aqueous phase environmental friendly organic corrosion inhibitors derived from one step multicomponent reactions: A review, *Journal of Molecular Liquids*, **2019**, 275, 18-40.
- [37] Goyal, M., Kumar, S., Bahadur, I., Verma, C., Ebenso, E.E., Organic corrosion inhibitors for industrial cleaning of ferrous and nonferrous metals in acidic solu-tions: A review, *Journal of Molecular Liquids*, **2018**, 256, 565-573.
- [38] Umoren, S.A., Eduok, U.M., Application of carbohydrate polymers as corrosion inhibitors for metal s ubstrates in different media: a review, *Carbohydrate Polymers*, **2016**, 140, 314-341.
- [39] Ufana Riaz, Chikezie Nwaoha, S.M. Ashraf, Recent advances in corrosion protective composite coatings based on conducting polymers and natural resource derived polymers, Progress in Organic Coatings, Volume 77, Issue 4, 2014.
- [40] A. Kalendová, I. Sapurina, J. Stejskal, D. Veselý: Anticorrosion properties of polyaniline-coated pigments in organic coatings, Corrosion Science 50 (2008) 3549-3551.
- [41] A. Kalendová, D. Veselý, I. Sapurina, J. Stejskal: Anticorrosion efficiency of organic coatings depending on the pigment volume concentration of polyaniline, Progress in Organic Coatings 63 (2008) 228-229
- [42] V.S. Jamadade, D.S. Dhawale: Studies on electrosynthesized leucoemeraldine and pernigraniline forms of polyaniline films and their supercapacitive behaviour, Synthetic Metals 160 (2010) 955–960.
- [43] Kalendová, A., Veselý. D., Kalenda, P., Properties of paints with hematite coated muscovite and talc particles, *Applied Clay Science*, **2010**, 48 (4), 581-588. doi.org/10.1016/j.clay.2010.03.007